FINITE ELEMENT SIMULATION OF GROWTH STRESS FORMATION AND RELATED BOARD DISTORTIONS RESULTING FROM SAWING AND FORCED DRYING*

SIGURDUR ORMARSSON†
Department of Applied Mechanics,
Chalmers University of Technology, SE-412 96, Göteborg, Sweden
and
School of Technology and Design,
Växjö University, S5 351 95 Växjö, Sweden

and MARIE JOHANSSON
Division of Structural Engineering,
Chalmers University of Technology, SE-412 96, Göteborg, Sweden

(Reveived for publication 1 November 2005; revision 13 March 2006)

ABSTRACT

Matching timber quality with end-user requirements is a major research issue and lack of straightness in timber is the most frequent complaint worldwide. The final distortion of timber boards is caused mostly by moisture-related deformations and growth stresses that develop during growth of the tree, but how much the growth rate and growth stresses affect the final shape stability is not fully understood. A finite element analysis in which stress development during tree growth was simulated was performed with the aim of better understanding how growth stresses are generated. The tree growth model was formulated in terms of large strain settings (large changes in volume), whereas the material model for stress development was based on the theory of small strains. An earlier three-dimensional distortion model was developed further for studying the influence of growth stresses on final distortion of the board. The results showed that growth stresses clearly vary during tree growth and they also form a large stress gradient from pith to bark. This itself can result in significant bow and crook deformation when the log is sawed into boards.

Keywords: tree growth; maturation strain; growth stress; wood; distortion.

---

* Based on a paper presented at IUFRO WP S5.01.04 Fifth Workshop on Wood Quality Modelling, 20–27 November 2005, Waiheke Island, New Zealand

† Corresponding author: sor@byg.dtu.dk

INTRODUCTION

Wood is a moisture sensitive, inhomogeneous, orthotropic material in which there often are internal stresses caused by biological maturation of the wood fibres. This state of stress can lead to board distortions directly after the logs are sawn. It can also influence distortions caused by changes in environmental conditions. Experimental studies have shown longitudinal growth stresses to vary markedly within a cross-section of an individual tree as well as between different trees of the same species and between trees of differing species (*see*, e.g., Archer 1986; Alhasani 1999). It is also known that both the growth stresses and the material properties of a tree are influenced by its growth rate (Archer 1986; Cown & Ball 2001). The stress state itself can also affect the growth rate (reaction wood) and the growth rate can influence the maturation strains that lead to growth stresses. Many complex biological and genetic properties affected by such factors as site conditions, climatic conditions, and silvicultural conditions can also have a strong influence on the growth rate of the tree. Much research has been conducted in this field (Larcher 1995; Kramer & Kozlowski 1979).

According to Plomion *et al*. (2001), the wood formation process is exceptionally complex and is far from being adequately investigated. Cell formation occurs in the cambium zone, which is made up of a layer of cells called the cambium initials. Both the wood (xylem) and the bark (phloem) cells are produced by division of these cambium initials. The formation process as a whole is driven by a large number of structural genes that govern cell-origination (by division), cell-differentiation, cell-maturation, cell-death, and heartwood formation. The cell wall consists of several layers (middle lamella, primary wall, and secondary wall) created at different periods during the differentiation process. At the beginning of this process, the middle lamella is developed further and the primary cell wall is formed (highly deformable and attached to the middle lamella). Thereafter, disposition of the secondary cell wall occurs, i.e., layers S1, S2, and S3 are formed. When cell maturation starts, firstly the cellulose material is laid down (crystallisation) and thereafter the lignin is produced and infiltrated into the newly formed cellulose material (lignification). These mechanisms are hypothesised to cause growth stresses to develop in the living tree. The disposition of lignin results in transversal expansion of the fibres (Boyd 1950), whereas crystallisation of the cellulose leads to longitudinal shrinkage of the wood cells (Bamber 1978). Since the maturing cells are attached to the old and already matured cells, a strain constraint develops in the stem; the maturing cells become stretched longitudinally and compressed tangentially, whereas the matured cells are exposed to the opposite stress conditions. During the progressive growth of a tree, the wood cells inside the trunk become increasingly compressed in the longitudinal direction. Various models based on the microstructure of the cell have been developed for analysing how the maturation

strains in wood cells are affected by the microfibril angle (*see* Yamamoto 1998; Guitard *et al*. 1999; Alméras *et al*. 2005). These models agree well with results of an experimental study on fibre level carried out by Yamamoto (1998).

Growth stresses at the cell level result in growth stress variation over the stem cross-section. One of the first to describe this variation was Kubler (1959a, b). Archer (1987) presented an analytical solution for growth stresses based on the assumption of axisymmetry. Several growth stress models for trees based on biological maturation strains have been reported (Archer & Byrnes 1974; Fournier *et al*. 1990; Skatter & Archer 2001; Fourcaud & Lac 2003). The authors used different types of finite elements in these works, i.e., axisymmetric solid elements, cylindrical shell elements, and multi-layer beam elements. Fourcaud *et al*. (2003) implemented the multi-layer beam model in the plant architecture simulation software AMAPpara. Experimental work has also been performed to confirm radial growth stress distributions (Archer 1986; Kubler 1987; Alhasani 1999; Raymond *et al*. 2004). A normal stem is subjected to longitudinal compression in the central parts and to longitudinal tension in the periphery. This stress state will cause deformation in material sawn from the stem. It has been shown experimentally that boards can have both spring and bow directly after sawing (Okuyama & Sasaki 1979; Mishiro & Booker 1988; Johansson & Ormarsson 2005). Simulation results of board distortion due to the redistribution of the growth stresses during sawing have also been presented by Constant *et al*. (1999).

In the present study, stresses in growing trees, board distortion due to stress relaxation that occurs during log sawing, and moisture-related distortions of timber boards were studied with numerical simulation. For problems of warping to be solved, it is important to determine the causes and learn how they can be reduced. Because of the complex structure of wood material, adequate analyses require the use of full three-dimensional simulation models in which the spatial material properties of the wood are incorporated (Ormarsson *et al*. 1998). It is assumed that the hypothesis at the micro-level can be extended to annual ring level (early/late wood). In addition, the processes causing cell death and heartwood formation are assumed to have no appreciable influence on the state of internal stress and development of material properties of the wood. Transient loads (e.g., from wind, snow, and water tension) and stress relaxation experienced during the tree's lifetime were not taken into account here.

MATERIALS AND METHODS

A three-dimensional simulation model for growth (maturation)-related stresses, linked with an already existing distortion model for timber products (Ormarsson 1999), was developed. The principal elements involved in simulating the entire chain of events from growth of the tree to obtaining the final timber product are

shown in Fig. 1. The growth stress model was a 3D-solid model in which the annual ring layers became progressively active during growth of the tree. The maturation strain was the driving force causing the growth stresses. The free maturation strain was defined on the basis of an experimental investigation of released maturation strain by Yamamoto (1998). All the material parameters were assumed to be fully developed during the differentiation period. Data on the history of the annual ring growth, the material orientation, and the gravity load represent further input data to the model. The distortion simulation consisted of two parts, one for simulating sawing of the log and the other for simulating drying distortion of the timber boards. The sawing of the log was simulated by removing thin elements from the model along the path of the saw blade. When the log was sawed into timber boards, the sawing caused a redistribution of the growth-stress field. The residual stresses in the boards were used as an initial stress field for the drying distortion model. The

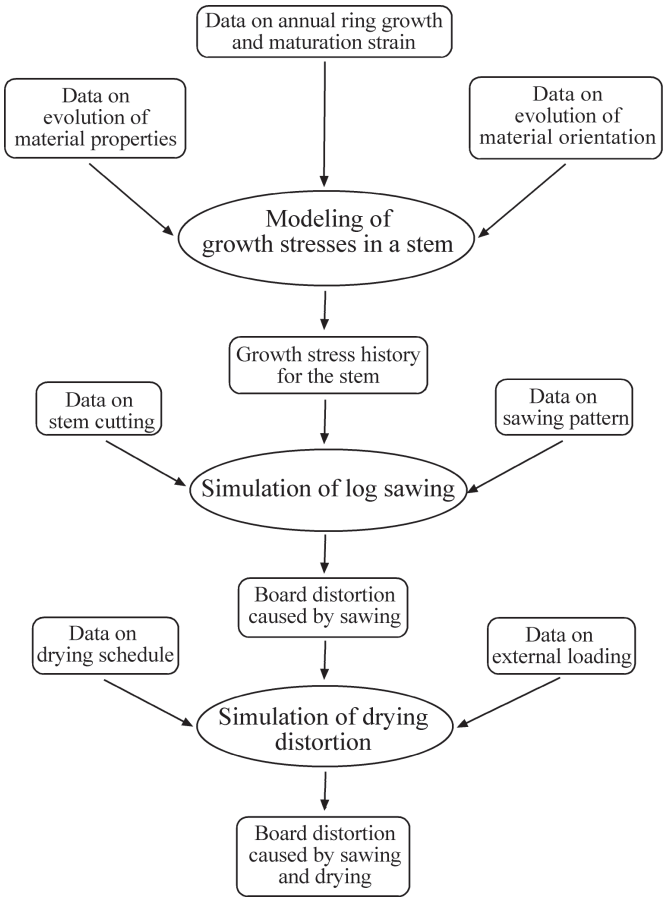

FIG. 1–Principal elements for the simulation of growth stresses and distortions in timber boards.

constitutive model used in the distortion model was a generalisation of models presented by Ranta-Maunus (1990) and Salin (1992) involving elastic, moisture-induced, and mechano-sorptive strains.

MATERIAL DATA

Stress simulation of tree growth differs significantly from applications in which the model geometry is defined from the start. The volume of the tree has to be created progressively during the analysis, all the material parameters and fibre orientations having to be determined progressively during the analyses as well. How the material properties mature during annual ring evolution has not yet been adequately investigated. The following sections describe how annual ring growth, stiffness properties, spiral grain, and maturation strains were determined in the present study on the basis of experimental work by Ormarsson & Cown (2005), Persson (2000), and Yamamoto (1998).

Annual Ring Growth and Density

The first input source needed for growth stress analysis is a history of progressive annual ring growth. These data have to be selected from experimental studies or from growth models based on climatic, biological, and genetic information. In the present study the criterion for annual ring growth was based on the experimental relationship between annual ring width and radial distance from the pith, as taken from Ormarsson & Cown (2005) for *Pinus radiata* D.Don. The surfaces used for annual ring evolution are shown in Fig. 2. The variable n is a ring number and g

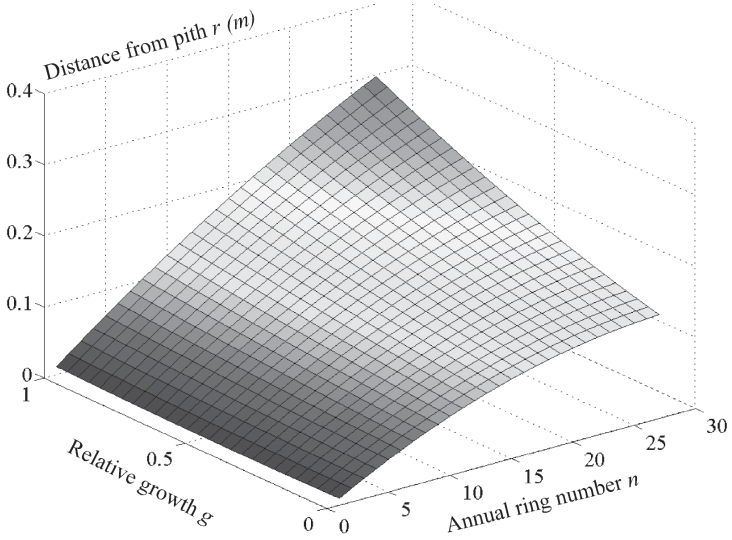

FIG. 2–Relationship between radial distance from the pith, ring numbers, and relative growth.

represents the index for relative growth varying between zero and one. The boundary values $g = 1$ and $g = 0$ represent the upper- and lower-limit curves for annual ring growth (Ormarsson & Cown 2005). With the help of this surface, an arbitrary annual ring growth can be determined. The expression for the surface is given in Eq. (1).

$$r = (10n - 14g - 0.17n^2 + 5ng + 12g^2 - 0.03n^2g - 1.2ng^2 + 0.1n^2g^2)*10^{-3} \quad (1)$$

With information concerning the distance from pith r and the relative growth g, all the material data needed (based on the curves presented by Ormarsson & Cown 2005) have been created. The expression for wood density is shown in Eq. (2), in which the density is assumed to decrease with increased growth rate.

$$\rho = 418.2 + 1623r - 24g - 1227rg - 48.4g^2 + 534rg^2 \quad (2)$$

Microfibril Angle and Spiral Grain Angle

For softwoods both the microfibril angle and spiral grain angle have a strong spatial variation inside the log (Cown *et al*. 1991, 2002; Säll 2002). The average general pattern for juvenile wood is for microfibril angle to decrease markedly in the radial direction but become more uniform in the mature wood. The maximum value for the spiral grain angle is that found close to the pith; in the radial direction from there it shows a rapid decrease. How these parameters are influenced by growth conditions is not well known. In the present study, however, it is assumed that both the microfibril and the spiral grain angle increase with growth rate. The expressions used here for the microfibril angle γ and the spiral grain angle θ are based on data presented by Ormarsson & Cown (2005) and given in Eq. (3) and (4). See also Fig. 3.

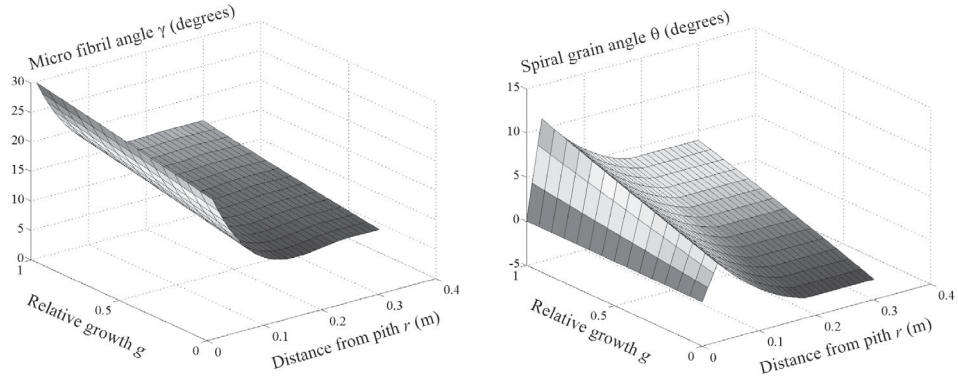

FIG. 3–Influence of distance from pith and of relative growth on the —
(a) micro-fibril angle γ (degrees)
(b) spiral grain angle θ (degrees).

$$\gamma = 26.1 - 259.7r + 6.4g + 1356r^2 + 13.9rg - 0.5g^2 - 2236.5r^3 - 191.9r^2g + 4.2rg^2 + 404r^2g^2 \quad (3)$$

$$\theta = \begin{cases} 144.36r + 251.34rg + 15.32rg^2 & for\ 0 \le r \le 0.027 \\ 5.9 - 78.8r + 6.9g + 171.9r^2 - 5.12rg + 0.6g^2 + 40r^2g - 7.08rg^2 & for\ r \ge 0.027 \end{cases} \quad (4)$$

Stiffness Parameters

In the present study all the stiffness parameters were assumed to have fully matured during the differentiation period, although another possibility would be to assume that these parameters increase during the maturation period, since the secondary cell wall is further modified during the lignification and the crystallisation processes. It is also well known that the parameters representing material stiffness and shrinkage are influenced by the annual ring width and the distance from the pith. The relationships used for the elastic moduli and the shear properties (in MPa) are shown in Eq. 5–10. These expressions are based on experimental data presented by Ormarsson & Cown (2005). Note that parameters such as Poisson's ratio are assumed to be independent both of growth conditions and of distance from the pith.

$$E_l = 8420 + 64530r - 2210g - 29490rg + 180g^2 + 3180rg^2 \quad (5)$$

$$E_r = 1020 + 6580r - 60g - 5560rg - 240g^2 + 2680rg^2 \quad (6)$$

$$E_t = 340 + 2230r - 10g - 1890rg - 100g^2 + 940rg^2 \quad (7)$$

$$G_{lr} = 1910 - 6250r - 440g + 29250r^2 + 3516rg - 40g^2 - 15260r^2g - 396rg^2 \quad (8)$$

$$G_{lt} = 1070 - 3610r - 280g + 17390r^2 + 2056rg - 9420r^2g - 216rg^2 \quad (9)$$

$$G_{rt} = 64 + 458r - 2g - 391rg - 20g^2 + 194rg^2 \quad (10)$$

Maturation Strain

To obtain reasonable simulation results for growth stresses it is important to have good experimental data for the maturation strains, since they serve as a driving force for growth stress development. The relationship between the so-called released maturation strains ξ_l and ξ_t and the microfibril angle γ, based on experimental work presented by Yamamoto (1998), is given in Eq. (11) and (12). Microfibril angle is strongly influenced by distance from the pith and slightly by the relative growth (Fig. 3a). On this basis, the maturation strains can be related to the relative growth and the distance from the pith (Fig 4).

$$\xi_l = (0.3675\gamma^2 - 4.675\gamma - 91.5)*10^{-3} \quad (11)$$

$$\xi_t = (-0.10071\gamma^2 + 1.1714\gamma + 88.9)*10^{-3} \quad (12)$$

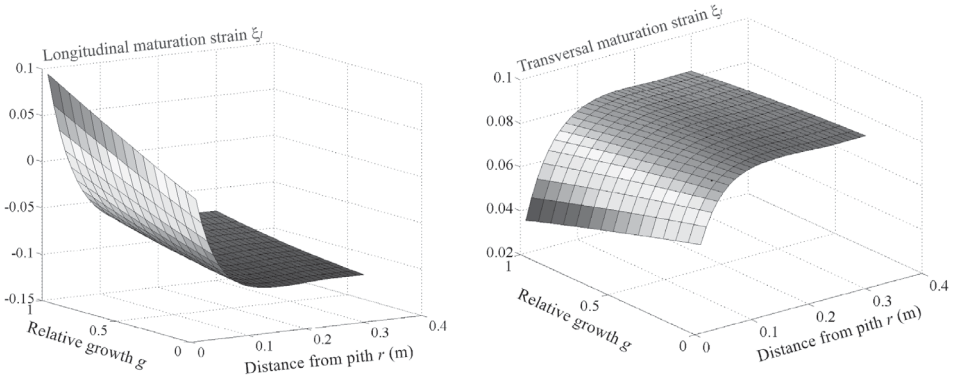

FIG. 4–Influence of distance from the pith and of relative growth on the —
(a) longitudinal maturation strain ξ_l (%)
(b) transversal maturation strain ξ_t (%).

Shrinkage Properties

For the growth stress model no further material parameters are needed, but for the distortion simulation shrinkage properties are defined by Eq. (13)–(15) (Ormarsson & Cown 2005). Because of a lack of information, such parameters as diffusion and mechanosorption were assumed to be independent of growth rate and distance from the pith.

$$\alpha_l = (16 - 166r + 22.9g + 464r^2 - 5.12rg - 9g^2 - 272r^2g + 69.12rg^2)*10^{-3} \quad (13)$$

$$\alpha_r = (63 + 450r + 41g - 748r^2 + 646.72rg - 22g^2 - 2359r^2g + 200.28rg^2)*10^{-3} \quad (14)$$

$$\alpha_t = (146 + 784r + 38g - 1781r^2 + 519.6rg + 4g^2 - 518r^2g - 121.6rg^2)*10^{-3} \quad (15)$$

MODELLING

The stress model consists of two major parts: a model for growth-related stresses, and a model for board distortions resulting from sawing of the log and changes in moisture content. These two models were linked together by transfer of the final stress state from the growth stress model to the distortion model as an initial stress field.

Growth Stresses

Generally, a three-dimensional continuum model for tree growth needs to take account of the longitudinal formation of the pith (and shoots); diametrical formation of the trunk (and branches); and progressive evolution of the material properties, the gravity load, the fibre orientation, and maturation strains. In the present model, the annual ring formation is formulated as a large volume extension based on the strain-displacement relationship for large deformations. The initial formation of

each annual ring occurs under stress-free conditions, through free enlargement in the radial and tangential directions. Next to the previous annual ring, these strains are zero, and show a linear increase during radial growth. During this period, all material properties, microfibril angles, and spiral grain angles are created on the basis of relative growth information and the annual ring number, as described in the section concerned with the data. The maturation process of the cell structure is assumed to start when the annual ring geometry, corresponding to fibre formation, is finished. The strains caused by cell maturation are modelled as shrinkage in the longitudinal fibre direction and swelling in the radial and tangential material directions. Evolution of these strains is based on Eq. (11) and (12). The tree goes into a winter period each year after the maturation of the respective annual ring. It is assumed that during this period of relative inactivity, no biological processes affecting stress occur. Cell death and heartwood formation are not taken into account in the model work.

The theory for tree growth was implemented into the commercial software ABAQUS by writing special user-routines for material behaviour, material orientation, and boundary conditions. The feature of adding new elements to the model was also used to simulate the progressive radial growth of the tree. The model employed is a full three-dimensional solid model able to take into account inhomogeneity in the material properties, material orientation, and maturation strains. The gravity load can also be added progressively when a new annual ring is created.

Cutting and Sawing of a Log

The cutting of stems into logs was simulated in such a way that the final growth stress state in the stem was used as an initial stress field for a new and appropriate log mesh (Fig. 5). This was implemented in ABAQUS by writing a user-routine for

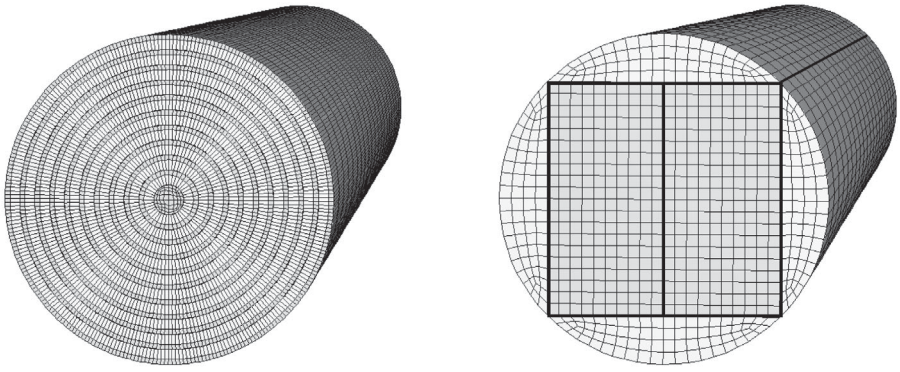

FIG. 5–Example of an element mesh —
(a) for simulating growth stresses
(b) for simulating cutting and sawing of the log.

initial stresses. In regions close to the ends of the log, significant stress redistribution occurs when the stress field is re-equilibrated because of the log cutting. In the next step, the log is sawn into several boards. This process is simulated by progressively removing thin layers of elements that represent the path of the saw blade. The redistribution of the stresses during the sawing can cause a significant deformation of individual boards, the extent of this depending on the stress state in the log and the sawing pattern used.

Moisture-related Distortion of Boards

To study how the residual growth stresses in the timber boards influence the drying distortion that occurs, the boards were further analysed under varying moisture conditions. The residual stresses in the sawn boards were used as an initial stress field for the distortion simulations. The drying model used was a three-dimensional finite element model for transient moisture flow (Ormarsson *et al*. 2002).

NUMERICAL RESULTS

On the basis of the input data detailed above, a three-dimensional simulation was performed to study how deformations and stresses develop during tree growth, sawing of the log, and drying of the boards.

Growth Stresses

To study the development of growth stresses, the growth of 20 annual rings was simulated in a small section of a stem. The piece was fixed at the bottom in the longitudinal log direction whereas the top end was free to move as a planar surface. Relative growth g was set to 0.2 for growth as a whole, growth thus being relatively slow. This resulted in a progressive reduction in growth rate over time (element mesh in Fig. 6). Variations in the longitudinal stress component along a radial path at four different ages are also shown in Fig. 6. Note that the stress distribution is due only to maturation of the cell, no creep or gravity load was included in the example. The free maturation strains used as a driving force for the growth stress development were based on experimental results (*see* Fig. 4). The results show that the inner core of the log becomes increasingly compressed during growth, whereas the tension stresses at the surface increase over time. The shape of the stress curves is influenced by the strong radial variation in maturation strains, material properties, spiral grain, and annual ring width. This radial stress variation can cause certain bow deformation of the boards after sawing.

Sawing of the Logs

The stresses contained in the growth stress model were transferred to the log model (different meshes) by means of stress functions based on results for the growth

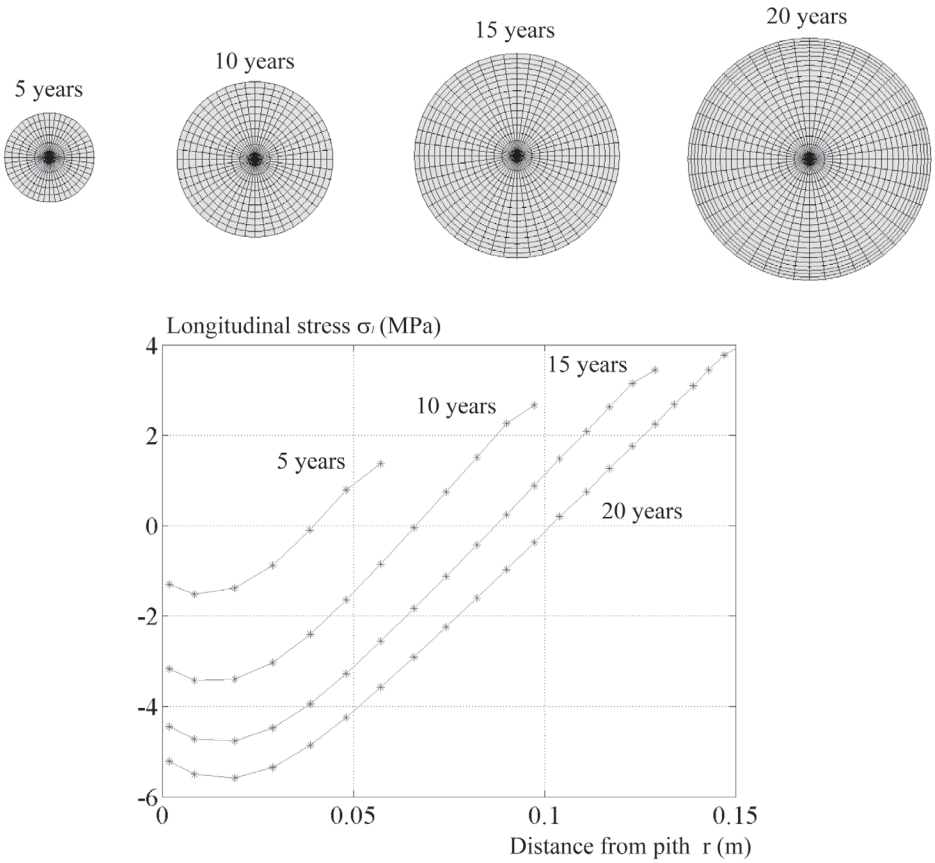

FIG. 6–How growth-related stresses in the longitudinal direction develop during tree growth

model. These functions were used as an initial stress field for the log model. An example of how the longitudinal growth stress field can change during cutting or sawing of a log is shown in Fig. 7. Initially, the log has compression stresses (~6 MPa) in the centre and tension stress (~4 MPa) in the periphery. When the stem is cut into logs, significant stress reduction occurs near the ends of the log. Sawing of the two outer-edge boards also causes significant stress redistribution that results in bow distortion in these thin boards. At the same time, the tension stresses increase at the surface of the log.

Drying Distortion of Boards

To study how growth stresses affect drying distortion (e.g., bow and twist), the log depicted in Fig. 7 was sawn into four flat-sawn boards. After sawing, the boards were exposed to drying from 27% m.c. down to about 10% mean m.c. The residual

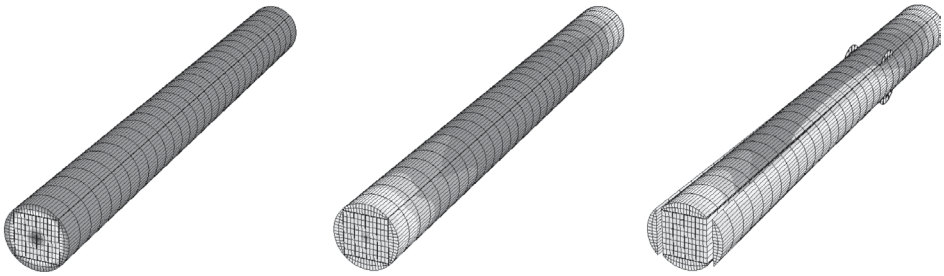

FIG. 7–Distribution of longitudinal growth stresses —
(a) in a long tree stem
(b) in a log after cutting
(c) in a log during sawing of the outer-edge boards.

growth stresses were used as initial stress data for the simulation. After sawing the boards showed only small stresses and slight (~2 mm) bow deformations (Fig. 8a), whereas after drying they were highly twisted (~6 degrees) and highly stressed (Fig. 8b). Note that the bow deformation after sawing was in the opposite direction from that after drying (~–3 mm). Cup deformation was not noticeable after sawing but became consideringly greater during drying.

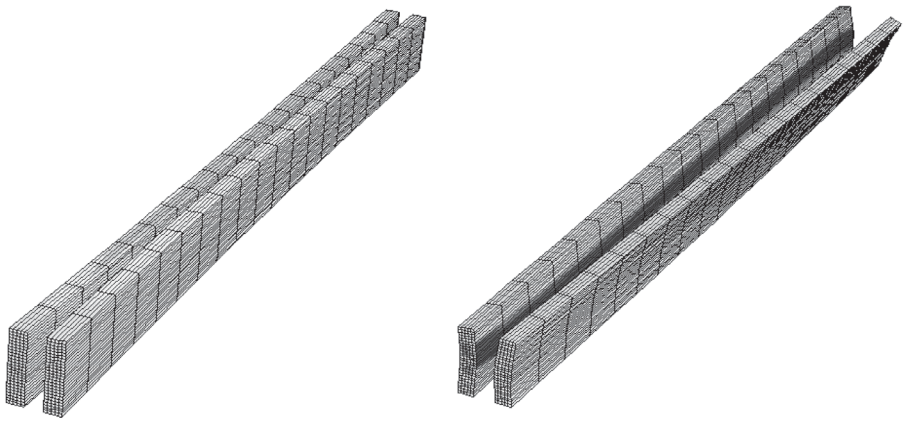

FIG. 8–Deformation and stress distribution —
(a) after sawing (a scale factor of 10)
(b) after drying (a scale factor of 5).

DISCUSSION AND CONCLUSIONS

Good knowledge of material properties, cell orientation, and maturation properties makes it possible to simulate the development of growth stresses during tree growth. The simulation showed a significant variation in longitudinal growth stresses from pith to bark. It also showed substantial changes in the stress profile

during growth, the inner core becoming increasingly compressed whereas the outer layer was subjected to increasing tension stresses. The shape of final stress pattern (Fig. 6) differs from the stress pattern presented by Skatter & Archer (2001) and Fourcaud *et al*. (2003). The reason for this difference was the strong radial variation in material properties, spiral grain, and maturation strains taken into account here. Ring width and stiffness of a new annual ring has a significant influence on how the stress field changes during the year.

The model was also used to study how the growth stress field influences board distortions caused by sawing and drying. The results show that a significant stress redistribution occurs during sawing of the log, resulting in clearly noticeable bow deformations, especially in the thin outer-edge boards. For symmetric sawing the growth stresses in the remaining centre are only slightly reduced and no bending distortion of the centre occurs. The bow deformation directly after sawing corresponds rather well with the experimental observations presented by Johansson (2002) and Johansson & Ormarsson (2005). Both the deformation after sawing and the remaining growth stresses in the stud influence deformation after drying. The deformation after sawing gives the stud an initial shape that will be added to the deformation due to drying. The growth stresses in the studs affect the drying stresses in terms of mechano-sorptive effect.

FUTURE WORK

The simulation model can be used to study how growth stresses and related distortions in wood are influenced by different wood properties and growth conditions. The model will be further developed so as to better take account of gravity load and external loadings through wind and snow. Since the trunk of the tree can be exposed to rather high loadings at some parts of the year, the growth stress model also needs to be expanded further to take account of creep strains. Creep can have a significant influence on the growth stress pattern. Trees that are exposed to abnormally high stress during growth begin to produce so-called reaction wood (compression or tension wood). This can happen, for example, when trees are exposed to high wind loads or when they grow on a steep slope. No really adequate criteria exist for determining when a tree starts to produce reaction wood, but there could be some history-based stress criterion for the most recently matured annual ring, for example. If some reasonable criterion for reaction wood were defined it could be added to the model, and then the growth rate for that region would need to be adjusted. Thus the cross-section of the trunk could change to a non-circular shape and all the material properties might need to be changed to values representing reaction wood. It is known that wood properties are often highly variable along a tree stem, so in future work this variation has to be taken into account in the growth stress model.

REFERENCES

ALHASANI, M.A 1999: Growth stresses in Norway spruce. Licentiate thesis, Report TVBK-1016, Lund University, Division of Structural Engineering, Lund, Sweden.

ALMÉRAS, T.; GRIL, J.; YAMAMOTO, H. 2005: Modelling anisotropic maturation strain in wood in relation to fibre boundary conditions, microstructure and maturation kinetics. *Holzforschung 59*: 347–353.

ARCHER, R.R. 1986: "Growth Stresses and Strains in Trees". Springer-Verlag, Berlin.

——1987: On the origin of growth stresses in trees. Part 1. Micromechanics of the developing cambial cell wall. *Wood Science and Technology 21*: 139–154.

ARCHER, R.R.; BYRNES, F.E. 1974: On the distribution of tree growth stresses. Part 1. An anisotropic plane strain theory. *Wood Science and Technology 8*: 184–196.

BAMBER, R.K. 1978: Origin of growth stresses. *Forpride Digest 8(1)*: 75–96.

BOYD, J.D. 1950: Tree growth stresses III. The origin of growth stresses. *Australian Journal of Scientific Research, B (biological Sciences) 3(3)*: 294–309.

CONSTANT, T.; ANCELIN, P.; FOURCAUD, T.; FOURNIER, M.; JAEGER, M. 1999: The French project SICRODEF: a chain of simulators from the tree growth to the distortion of boards due to the release of growth stresses during sawing. *In* Workshop IUFRO S5.01-04 – La Londe-Les-Maures, 5–12 September.

COWN, D.J.; BALL, R. 2001: Wood densitometry of 10 *Pinus radiata* families at seven contrasting sites: influence of tree age, site, and genotype. *New Zealand Journal of Forestry Science 31(1)*: 88–100.

COWN, D.J.; YOUNG, G.D.; KIMBERLEY, M.O. 1991: Spiral grain patterns in plantation-grown *Pinus radiata*. *New Zealand Journal of Forestry Science 21(2/3)*: 206–216.

COWN, D.J.; BALL, R.D.; RIDDELL, M.; WILCOX, P. 2002: Microfibril angle in plantation pine: distribution and relative influence on product performance. *In* Proceedings "Connection between Forest Resources and Wood Quality: Modelling Approaches and Simulation Software", 4th IUFRO Workshop, Harrison Hot Springs, BC, Canada, September. 14 p.

FOURCAUD, T.; LAC, P. 2003: Numerical modelling of shape regulation and growth stresses in trees. I. An incremental static finite element formulation. *Trees 17*: 23–30.

FOURCAUD, T.; BLAISE, F.; LAC, P.; CASTÉRA, P.; de REFFYE, P. 2003: Numerical modelling of shape regulation and growth stresses in trees, II. Implementation in the AMAPpara software and simulation of tree growth, Trees. 17:31-39.

FOURNIER, M.; BORDONNE, P.A.; GUITARD, D.; OKUYAMA, T. 1990: Growth stress patterns in tree stems. *Journal of Wood Science and Technology 24*: 131–141.

GUITARD, D.; MASSE, H.; YAMAMOTO, H; OKUYAMA, T. 1999: Growth stress generation: a new mechanical model of the dimensional change of wood cells during maturation. *Journal of Wood Science and Technology 45*: 384–391.

JOHANSSON, M. 2002: Moisture-induced distortion in Norway spruce timber — experiments and models, Doctoral thesis, Publ. 02:3, Chalmers University of Technology, Department of Structural Engineering: Steel and Timber Structures, Göteborg, Sweden.

JOHANSSON, M.; ORMARSSON, S. 2005: Effect of residual stresses on performance of sawn timber — experiments. Presented at IUFRO WP S5.01.04 Fifth Workshop on Wood Quality Modelling, 20–27 November, Waiheke Island, New Zealand.

KRAMER, P.J.; KOZLOWSKI, T.T. 1979: "Physiology of Wood Plants". Academic Press, London.

KUBLER, H. 1959a: Studies on growth stress in trees — part I: The origin of growth stresses and the stresses in Transverse Direction [Studies über Wachstumsspannung des Holzes - Erste Mitteilung: Die Ursache der Wachstums-spannungen und die Spannungen quer zur Faserrichtung - in German]. *Holz als Roh- und Werkstoff 17(1)*: 1–9.

——1959b: Studies on growth stress in trees — part II: Longitudinal stresses [Studies über Wachstums-spannung des Holzes - Zweite Mitteilung: Die Spannungen in Faserrichtung - in German]. *Holz als Roh- und Werkstoff 17(2)*: 44–54.

——1987: Growth stresses in trees and related wood properties. *Forest Products Abstracts 10(3)*: 62–119.

LARCHER, W. 1995: "Physiological Plant Ecology: Ecophysiology and Stress Physiology of Functional Groups", third edition. Springer-Verlag, Berlin.

MISHIRO, A.; BOOKER, R.E. 1988: Warping in new crop radiata pine 100 × 50 mm (2 by 4) boards. *Bulletin of the Tokyo University Forests 80*: 37–68.

OKUYAMA, T.; SASAKI, Y. 1979: Crooking during lumbering due to residual stresses in the tree. *Mokuzai Gakkaishi 25(11)*: 681–687.

ORMARSSON, S. 1999: Numerical analysis of moisture-related distortion in sawn timber. Doctoral thesis, Publ. 99:7, Chalmers University of Technology, Department of Structural Mechanics, Göteborg, Sweden.

ORMARSSON, S.; COWN, D. 2005: Moisture-related distortion of timber boards of radiata pine: comparison with Norway spruce. *Wood and Fiber Science 37(3)*: 424–436.

ORMARSSON, S.; DAHLBLOM, O.; PETERSSON, H. 1998: A numerical study of the shape stability of sawn timber subjected to moisture variation, Part 1: Theory. *Wood Science and Technology 32*: 325–334.

ORMARSSON, S.; PETERSSON, H.; DAHLBLOM, O. 2002: Finite element simulations of moisture transport and moisture related warping in wooden products. *In* Fifth World Congress on Computational Mechanics, Vienna, Austria, 7–12 July. 11 p.

PERSSON, K. 2000: Micromechanical modelling of wood and fibre properties. Doctoral thesis, Publ. TVSM-1013, Division of Structural Mechanics, Lund University, Sweden.

PLOMION, C.; LEPROVOST, G.; STOKES, A. 2001: Wood formation in trees. *Plant Physiology 127*: 1513–1523.

RANTA-MAUNUS, A. 1990: Impact of mechano-sorption creep to the long-term strength of timber. *Holz als Roh- und Werkstoff 48*: 67–71.

RAYMOND, C.A.; KUBE, P.D.; PINKARD, L.; SAVAGE, L.; BRADLEY, A.D. 2004: Evaluation of non-destructive methods of measuring growth stress in *Eucalyptus globulus*: relationships between strain, wood properties and stress. *Forest Ecology and Management 190*: 187–200.

SALIN, J.G. 1992: Numerical prediction of checking during timber drying and a new mechano-sorptive creep model. *Holz als Roh- und Werkstoff 50*: 195–200.

SÄLL, H. 2002: Spiral grain in Norway spruce. Doctoral thesis, No 22, Växjö University, Wood Design and Technology, Växjö, Sweden.

SKATTER, S.; ARCHER, R.R. 2001: Residual stresses caused by growth stresses within a stem with radially varying spiral grain angle — two numerical solution approaches: 1) finite element method and 2) transfer matrix method. *Wood Science and Technology 35*: 57–71.

YAMAMOTO, H. 1998: Generation mechanism of growth stresses in wood cell walls: roles of lignin deposition and cellulose microfibril during cell wall maturation. *Wood Science and Technology 32*: 171–182.